

서식 있음: 글꼴: (한글) 맑은 고딕,
(한글) 한국어

Analytic and Experiment Investigation on the Crosstalk Elimination of Resistive Sensor Array based pressure mapping System

Z.Y.Mao¹, P.Cai^{1*} and X.Y.Peng¹

¹ Department of Instrument Science and Engineering Shanghai Jiaotong University, Shanghai, People's Republic of China, 200240
Corresponding Author / E-mail: pcai@sjtu.edu.cn, TEL: +86-21-342-04003, FAX: +86-21-342-04003

서식 있음: 위치: 가로: 가운데,
기준: 여백, 세로: 0.11 글자, 기준:
단락, 텍스트 배치: 둘러싸기

KEYWORDS : resistive sensor array , crosstalk , ratio measurement , zero potential circuit , on-resistance

For a resistive sensor array based pressure mapping system, the critical issue is to eliminate the crosstalk caused by row wise and column wise electric inter-connection among respective row elements and column elements. In this study, based on the analysis on the influence mechanism of crosstalk, an improvement to the zero potential circuit approach is presented. Then the interference of inter-resistance among rows or columns is discussed. After that, the crosstalk errors of the circuits are evaluated and compared in experiment. . We revealed the relation between the spatial resolution of array and crosstalk errors by experimental study. The results of analysis and the experiment results agree with each other.

Manuscript received: January XX, 2011 / Accepted: January XX, 2011

two methods, but they only investigated the circuit by simulation and little attention is made on the error caused by inter-row or inter-column resistance. Usually, the evaluation about the crosstalk on experiment basis is more instructive than simulation for us to select appropriate pressure mapping system for pressure distribution measurement.

This study analyzes the crosstalk on experiment basis and an improvement to the zero potential circuit approach is made based on ratio measurement technique for further decrement of the crosstalk, and an experimental research was undertaken to reveals the relation between the errors and the special resolution of resistive sensor arrays.

In our pressure mapping system, the contact force sensor arrays include two sets of parallel electrodes which are each formed on a thin, flexible supporting sheet. The electrodes are separated by a pressure sensitive resistive coating. Two such electrodes are placed orthogonally to each other, thus building a matrix of sensors or pressure pad. The resistance between electrode intersections changes as pressure is applied on it.

The pressure distribution is obtained by scanning the sensor array and measuring the resistance variation of each element. Since the unselected elements are also electrically connected via parasitic path as the row and column electrodes format is applied, the crosstalk occurs. The crosstalk mechanism can be analyzed with Fig.2, where, for simplicity, only a small portion of the array is presented (2 rows

1. Introduction

The high spatial resolution measurement of bare-foot plantar pressure distribution is of great important to the biomedical and the evaluation of body balance function and rehabilitation of lower-limb disabled sufferers, because the pressure characterization (such as peak point and center of pressure trajectory and so on) in different regions of the foot may help to reveal the causes of dysfunction. For a resistive sensor array based pressure mapping system, which is generally composed of several thousands of resistive sensor for acquiring sufficient spatial resolution, the critical issue is to eliminate the crosstalk caused by row-wise and column-wise electric inter-connection among respective row elements and column elements.

Several researches have been carried out on the way to eliminate the crosstalk in recent years, of which the voltage feedback [1,2] and zero potential [3,4] method are commonly used one. Tommaso D'Alessio[5] and Hong Liu[6] made some comparison between the

and 2 columns)

When the resistance R_{ij} is to be read, the current cross not only R_{ij} , but also the parasitic paths composed of the surrounding three resistive $R_{i,j-1}, R_{i+1,j-1}$ and $R_{i+1,j}$ in series (Fig.2). So, the crosstalk arises when attempting to read the voltage corresponding to one assigned element.

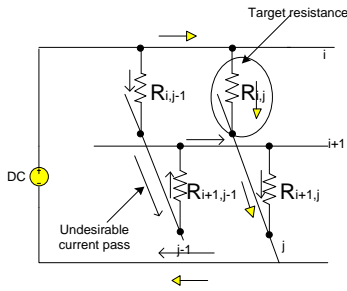


Fig. 1 Crosstalk analysis

Zero potential circuit restrains the crosstalk [3,4] by taking scanned rows floating and connecting non-scanned rows to the ground. But they neglected the influence of the on resistance of multiplexers. There exists crosstalk when the on resistance of the multiplexer cannot be neglected compared with the resistance of the pressure sensing element.

2 An improvement to the zero potential circuit

By taking the practical exciting voltage as the reference voltage of A/D converter, the influence of the on resistance of the multiplexer can be restrained. Fig.2 shows the schematic diagram of the improved zero potential circuit. The exciting voltage V_E of the sensor array is connected to the In-port of the mux1 and the voltage V_e of the out-port of the mux1 is the practical exciting voltage of the under test device (UTD). As the exciting voltage of the i th-row is the same as the reference voltage of the ADC, then the readout of the ADC will be irrelevant to the equivalent shunt resistance. Thus, by taking the advantage of ratio measurement technology, the crosstalk is offset.

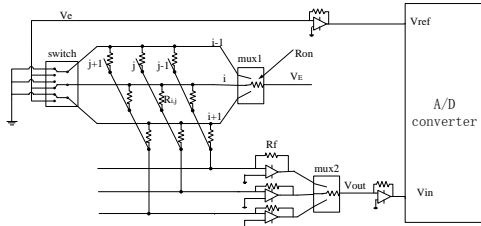


Fig.2 Schematic diagram of the improved zero potential circuit

Under ideal conditions, the output voltage of the operational amplifier can be written as:

$$V_{out} = V_E \times \frac{R_f}{R_{ij}} \tag{1}$$

But the existence of on-resistance of the multiplex, then, the output voltage can be written as:

$$V_{out} = V_E \frac{R_{\Sigma}/R_{ij}}{R_{on} + R_{\Sigma}/R_{ij}} \times \frac{R_f}{R_{ij}} \tag{2}$$

Where R_{Σ} is the equivalent resistance of the parasitic paths. Fig.3 shows the equivalent circuit of improved method.

we also have:

$$V_e = V_E \times \frac{R_{\Sigma}/R_{ij}}{R_{on} + R_{\Sigma}/R_{ij}} \tag{3}$$

So, the output of the ADC can be expressed as

$$N = \frac{V_{out}}{V_e} * 2^n = \frac{R_f}{R_{ij}} * 2^n \tag{4}$$

Where n stand for resolution of ADC, when supposed that R_f, R_{on} and n are constant, it can be seen that the result of the ADC is only depend on R_{ij} , while independent of R_{Σ} .

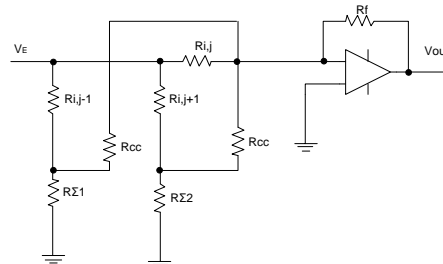


Fig.3 Equivalent circuits

To evaluate the effect of ratio measurement, we constructed a resistive array including 16 rows and 16 columns with metal film resistors. Four different resistance values (10kΩ, 20kΩ, 30kΩ, 40kΩ) were adopted to form four sub arrays, each of which comprise 8×8 elements. In each sub array, one resistance was selected as the UTD R_{ij} , we select six different resistances as R_{ij} .

Fig.4 shows the relative errors when the reference voltage of A/DC is a fixed value. Where the exciting voltage is set to be 1V, and feedback resistance R_f as 10kΩ. The errors is defined as:

$$errors(\%) = \frac{V_{single} - V_{out}}{V_{single}} * 100\% \tag{5}$$

where V_{single} is the voltage which would be read when only R_{ij} is connected, and V_{out} is the output voltage when R_{ij} place in resistance arrays.

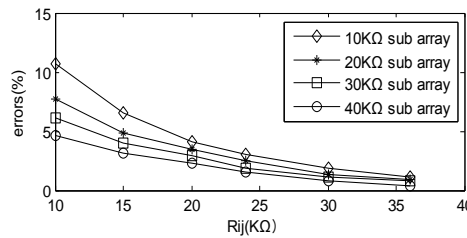


Fig.4 Relative error when the reference voltage of ADC is fixed

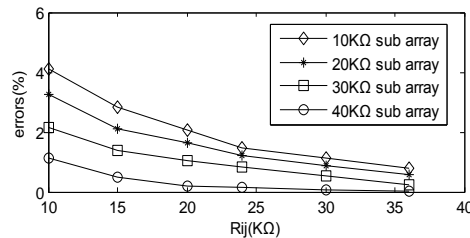


Fig.5 Relative error when the reference voltage of ADC is varied with R_{Σ}

Fig.5 shows the errors used the improved zero potential circuit. Comparing Fig.5 with 4, we can find that the errors have notably reduced.

3. The influence of inter-row and inter-column resistance

Because the pressure sensitive resistive coating is coated continuously, there are inter-row resistance R_{rr} and inter-column resistance R_{cc} as shown in Fig.6. According to circuit shown in Fig.2, current flowing through the inter-row resistance will not affect the measurement, because one end of inter-row resistance is virtual ground. But the inter-column resistance will affect the measurement. Because that shunt path would affect the output of the circuit when current through inter-column resistance R_{cc} .

Fig.7 shows the equivalent circuits of the resistive sensor array when the inter-column resistance is taken into consideration. Generally, the main affect are the adjacent column R_{ij+1} while R_{ij-1} , and other inter-column resistance can be neglected when scanning $R_{i,j}$. Then, the output voltage can be written as:

$$V_{out} = V \left(\frac{R_{\Sigma 1} // R_{cc}}{R_{ij-1} + R_{\Sigma 1} // R_{cc}} \times \frac{R_f}{R_{cc}} + \frac{R_{\Sigma 2} // R_{cc}}{R_{ij+1} + R_{\Sigma 2} // R_{cc}} \times \frac{R_f}{R_{cc}} + \frac{R_f}{R_{ij}} \right) \quad (6)$$

Where $R_{\Sigma 1}$ is the resistance $R_{1,j-1} // R_{2,j-1} // \dots // R_{i-1,j-1} // R_{i+1,j-1} \dots // R_{n,j-1}$.

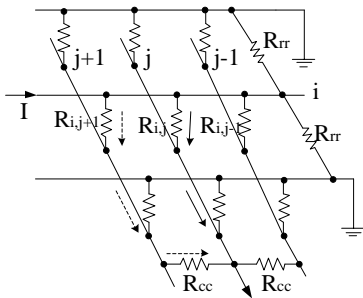


Fig.6 Schematic diagram on inter-row and inter-column interference

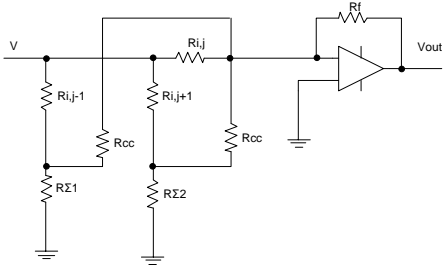


Fig.7 Equivalent circuits of inter-column interference

Suppose that $R_{ij-1} = R_{ij+1} = R_0$, and $R_{\Sigma 1} = R_{\Sigma 2} = R_{\Sigma 0}$.

The errors can be written as:

$$\text{errors}(\%) = \frac{2 \times R_{i,j} \times R_{\Sigma 0}}{R_0 \times (R_{\Sigma 0} + R_{cc}) + R_{\Sigma 0} \times R_{cc}} \times 100\% \quad (7)$$

It can be found from Equations (7) that the errors will decrease by reduce the value of $\frac{R_{i,j}}{R_{cc}}$. The value of $\frac{R_{i,j}}{R_{cc}}$ represents the ratio between resistance of sensing element and inter-column Ohm resistance of the coating material. Under ideal conditions, $R_{cc} \gg R_{i,j}$ but in practice $R_{cc} \approx 10^1 \sim 10^3 R_{i,j}$. To decrease practical errors, we can add a single-pole single-throw switch in all columns and connect the non-scanning rows to ground.

The error caused inter-column resistance can be evaluated by adding inter-column resistance in the discrete resistor arrays. In our experiment $R_{i,j} = 5k\Omega$, and the other resistors in i th-row resistance is $100 k\Omega$, and other surround resistance is $1 M\Omega$, $R_{cc} = 10k\Omega \sim 1000k\Omega$. Fig.9 shows the results, the dotted line indicates measurement curve, and real line indicates the ideal curve. The ideal curve can be written as:

$$\text{errors}(\%) \approx \frac{1}{K+10} \times 100\% \quad (8)$$

where $K = \frac{R_{cc}}{R_{i,j}}$.

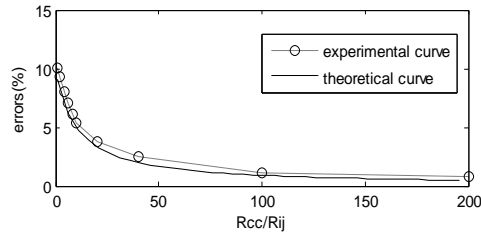


Fig.8 The influence of inter-resistance on errors

From Fig.8, we can conclude that the measurement value agree with the theoretical value, and if the relative error is expected to be less than 1%, The inter-column Ohm resistance of the coating material should be 100 times greater than resistance of sensing element.

4 Spatial resolution and measurement

To achieve fine pressure mapping high spatial resolution is expected. But higher spatial resolution results in poor measurement accuracy. The spatial resolution of a resistance arrays is equivalent to the numbers of array elements in unit area. So, three to sixteen scale resistance arrays are designed to study the impact of spatial resolution of arrays. The resistance in the array was selected as $10k\Omega$.

According to analysis (referring to Fig.3), the relation between errors and array scale could be solved as follow:

$$R_{\Sigma} = \frac{N}{(N-1)^2} R \quad (9)$$

$$\begin{aligned} \text{errors}(\%) &= \frac{R_{on}}{R_{on} + R_{\Sigma} // R_{ij}} \times 100\% \quad (10) \\ &= \frac{R_{on}}{R_{on} + \frac{10N}{(N-1)^2 + N}} \times 100\% \end{aligned}$$

where N indicate the scale of resistance arrays. When R_{on} is constant, there are approximately linearly proportional between errors and N.

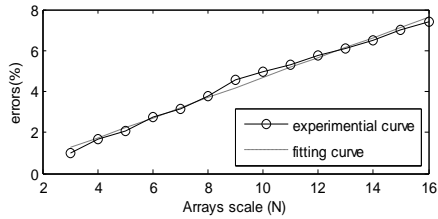


Fig.9 The influence of spatial resolution of a resistor array
Fig.9 shows the result of a measurement, while $R_{on} = 100\Omega$. From the curve, we can find that the values for the errors are assumed to be approximately linearly proportional to the scale of resistance arrays, these agree with Equation (10).

The spatial resolution of arrays can be written as:

$$\rho = P \times N^2 \quad (11)$$

where, ρ indicate the spatial resolution, and P is a constant.

It can be found from Equations (11) that, the values of the errors and the spatial resolution of arrays perform the power function relationship.

We constructed an applicable pressure mapping system with the off-the-shelf pressure pad as shown in Fig.10. Fig.10(a) show the measurement system of planta pressure distribution and (b) show the nephogram of pressure distribution.

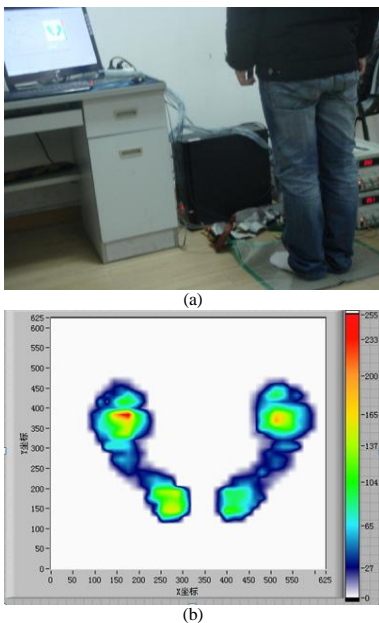


Fig.10 (a) Pressure mapping system. (b) nephogram of pressure distribution

The pressure mapping system is composed of thin film pressure pad which include 40 rows and 40 columns, the scanning control circuit, and data acquisition and processing system.

By the variety of the spatial resolution of array, the relative error is measured respectively.

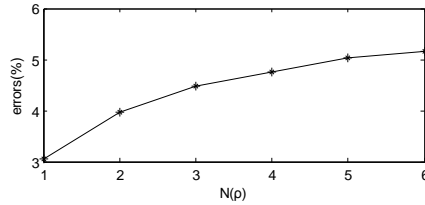


Fig.11 The influence of spatial resolution of a practical pressure mapping system

Fig.11 shows that the errors will increase as the expansion of the spatial resolution from ρ to 6ρ . Although, the spatial resolution will be improved if increase the density of contact sensors arrays, there also increase crosstalk. So, it is important to consider harmonic spatial resolution and precision when select pressure distribution measurement system.

5. Conclusions

In this study, an effective approach to reduce the influence of the crosstalk has been designed, and experiment results have demonstrated the feasibility. The relation between the spatial resolution of array and crosstalk related measurement error has been investigated. The results of analysis and the experiment results agree with each other. The influence of inter-rows or inter-columns resistance is also discussed, and it is concluded that the inter-resistance between two adjacent rows or columns should be 100 times greater than that of the sensing element if the relative error is limited to 1%. Based on above analysis and design, a practical pressure mapping system is constructed, and it demonstrates satisfactory measurement conformability.

ACKNOWLEDGEMENT

The research was supported by National Science and Technology Support Project "Balance Function Evaluation and Rehabilitation Training System and Its Clinical applications for Lower Limb Disabled" (2009BAI71B06).

REFERENCES

- [1]M. Witte, A. Mitchell "Tactile sensing system device for robotic manipulation" IEEE International Workshop on Intelligent Motion Control pp.893-896 1990
- [2]Makoto SHIMOJO "A Flexible High Resolution Tactile Imager with Video Signal Output" International Conference on Robotics and Automation 1991
- [3]M. Shimojo, A. Namiki, M. Ishikawa, R. Makino, K. Mabuchi," A tactile sensor sheet using pressure conductive rubber with electrical-wires stitched method" IEEE Sensors Journal 4 pp.589-596 2004
- [4]R.S. Saxena "A new discrete circuit for readout of resistive sensor arrays" Sensor and Actuator A: physical Vol.149, No.1, pp.93-99, 2009
- [5]Tommaso D'Alessio "Measurement errors in the scanning of piezoresistive sensors arrays" Sensor and Actuator A: physical Vol.72, No.1, pp.71-76, 1999
- [6]Hong Liu, Yuan-Fei Zhang, Yi-Wei Liu, Ming-He Jin "Measurement errors in the scanning of resistive sensor arrays" Sensor and Actuator A: physical Vol.163, No.1, pp.198-204, 2010